Oncogene goosecoid is transcriptionally regulated by *E2F1* and correlates with disease progression in prostate cancer

Yue Ge[1], Sheng Ma[1], Qiang Zhou[2], Zezhong Xiong[1], Yanan Wang[1], Le Li[1], Zheng Chao[1], Junbiao Zhang[1], Tengfei Li[1], Zixi Wu[1], Yuan Gao[1], Guanyu Qu[1], Zirui Xi[1], Bo Liu[3], Xi Wu[4], Zhihua Wang[1]

[1]Department of Urology, Tongji Hospital, Tongji Medical College, Huazhong University of Science and Technology, Wuhan, Hubei 430030, China;
[2]Department of Urology, Qinghai University Affiliated Hospital, Qinghai University Medical College, Xining, Qinghai 810001, China;
[3]Department of Oncology, Tongji Hospital, Tongji Medical College, Huazhong University of Science and Technology, Wuhan, Hubei 430030, China;
[4]Department of Urology, First Hospital of Laohekou City, Xiangyang, Hubei 441800, China.

Abstract

Background: Although some well-established oncogenes are involved in cancer initiation and progression such as prostate cancer (PCa), the long tail of cancer genes remains to be defined. Goosecoid (*GSC*) has been implicated in cancer development. However, the comprehensive biological role of *GSC* in pan-cancer, specifically in PCa, remains unexplored. The aim of this study was to investigate the role of *GSC* in PCa development.

Methods: We performed a systematic bioinformatics exploration of *GSC* using datasets from The Cancer Genome Atlas, Genotype-Tissue Expression, Gene Expression Omnibus, German Cancer Research Center, and our in-house cohorts. First, we evaluated the expression of *GSC* and its association with patient prognosis, and identified *GSC*-relevant genetic alterations in cancers. Further, we focused on the clinical characterization and prognostic analysis of *GSC* in PCa. To understand the transcriptional regulation of *GSC* by E2F transcription factor 1 (*E2F1*), we performed chromatin immunoprecipitation quantitative polymerase chain reaction (qPCR). Functional experiments were conducted to validate the effect of *GSC* on the tumor cellular phenotype and sensitivity to trametinib.

Results: *GSC* expression was elevated in various tumors and significantly correlated with patient prognosis. The alterations of *GSC* contribute to the progression of various tumors especially in PCa. Patients with PCa and high *GSC* expression exhibited worse progression-free survival and biochemical recurrence outcomes. Further, *GSC* upregulation in patients with PCa was mostly accompanied with higher Gleason score, advanced tumor stage, lymph node metastasis, and elevated prostate-specific antigen (PSA) levels. Mechanistically, the transcription factor, *E2F1*, stimulates *GSC* by binding to its promoter region. Detailed experiments further demonstrated that *GSC* acted as an oncogene and influenced the response of PCa cells to trametinib treatment.

Conclusions: *GSC* was highly overexpressed and strongly correlated with patient prognosis in PCa. We found that *GSC*, regulated by *E2F1*, acted as an oncogene and impeded the therapeutic efficacy of trametinib in PCa.

Keywords: Goosecoid; Prostate cancer; Prognosis; E2F transcription factor 1; Trametinib

Introduction

Prostate cancer (PCa), which accounts for a significant number of cancer-related deaths in men worldwide,[1,2] follows a sequential progression from prostate intraepithelial neoplasia to adenocarcinoma and metastatic disease.[3] The development of PCa is influenced by genetic changes, particularly mutations in oncogenes and tumor suppressor genes.[4–6] Phosphatase and tensin homolog (*PTEN*) loss and hyperactivated phosphatidylinositol-3-hydroxykinase/protein kinase B (PI3K/AKT) signaling are recognized as key drivers of PCa pathogenesis.[7] Additionally, *BRCA1/BRCA2* are essential for maintaining genomic stability and repairing damaged DNA. Therefore, mutations of *BRCA1/BRCA2* may contribute to the progression of PCa.[8] Despite significant advancements in understanding the mechanisms underlying PCa development, the reason why a small subset of patients with PCa experience rapid progression and poor prognosis remains to be fully elucidated.[4] Therefore, there is an urgent need to identify promising biomarkers for PCa prognosis.

Access this article online

Quick Response Code:

Website: www.cmj.org

DOI: 10.1097/CM9.0000000000002865

Yue Ge and Sheng Ma contributed equally to this work.

Correspondence to: Dr. Xi Wu, Department of Urology, First Hospital of Laohekou City, Xiangyang, Hubei 441800, China
E-Mail: wuxi227@aliyun.com;
Dr. Zhihua Wang, Department of Urology, Tongji Hospital, Tongji Medical College, Huazhong University of Science and Technology, Wuhan, Hubei 430030, China
E-Mail: zhwang_hust@hotmail.com

Chinese Medical Journal 2024;137(15)
Received: 26-06-2023; **Online:** 24-11-2023 **Edited by:** Yuanyuan Ji

Goosecoid (*GSC*) is a conserved transcription factor[9] that plays a crucial role in embryonic development, particularly in gastrulation[10,11] and neural crest[12] formation. Accumulating evidence has suggested that *GSC* shows significant effects on tumor migration and invasion,[9,13] and it is highly associated with multiple metastasis-related biological processes, including epithelial-mesenchymal transition, transforming growth factor (TGF)-β, and Wnt/β-catenin signaling pathways.[14–16] These findings strongly indicate the involvement of *GSC* in malignant tumor progression. Consistent with this, strong evidence indicates a poorer prognosis for patients with high *GSC* expression in different types of tumors, including ovarian, liver, and breast cancer.[9,13,14] Although prior studies on PCa have shown that *GSC* expression is influenced by downstream methylation and the cyclin D1 network,[17,18] it remains unclear whether different clinical stages and outcomes are associated with *GSC* in PCa, requiring further investigation.

In this study, we conducted a comprehensive bioinformatics analysis to investigate the biological roles and prognostic importance of *GSC* in various tumors with a particular focus on PCa. The functional significance of alterations in *GSC* expression in PCa was systematically investigated in relation to prognosis, genetic alterations, immune cell infiltration, and drug responses. Our analysis revealed that *GSC* was the top-ranking gene concerning genetic alterations. We performed detailed *in vitro* and *in vivo* experiments to elucidate the oncogenic functions of *GSC* in PCa.

Methods

Analysis of GSC expression

Genome-wide mRNA expression data for 33 types of cancer in The Cancer Genome Atlas (TCGA) cohort were obtained from the University of California, Santa Cruz (UCSC) Cancer Genomics Browser (https://genome-cancer.ucsc.edu/). We used the Tumor Immune Estimation Resource 2.0 (TIMER2) website (http://timer.cistrome.org/) to compare *GSC* expression between tumors and adjacent tissues in the TCGA cohort.[19] Additionally, we utilized SangerBox (http://SangerBox.com/Tool) to analyze the expression of *GSC* in tumors and their corresponding normal tissues by combining the TCGA and Genotype-Tissue Expression (GTEx) cohorts.

Survival prognosis analysis

To retrieve the overall survival (OS) and progression-free survival (PFS) data from the TCGA database, we accessed the UCSC online website. The tumor patients were divided into high and low *GSC* expression groups based on the median *GSC* expression. Kaplan–Meier survival plots for various tumors were generated using the R package "survival". We used the log-rank test to compare survival curves and performed Cox regression analysis to calculate the hazard ratio (HR) using the SangerBox online platform.

In addition, we obtained RNA-Sequence data and the corresponding clinical data for 105 PCa samples from the German Cancer Research Center (Deutsches Krebsforschungszentrum, DKFZ) cohort using the cBioPortal for Cancer Genomics (http://cbioportal.org).[20,21] We used R studio (https://www.r-project.org/) to analyze the relationship between *GSC* expression and biochemical recurrence (BCR) in patients with PCa. We also analyzed the differences in *GSC* expression among PCa patients with different clinical characteristics, such as T stage, N stage, and Gleason scores. For all statistical analyses, a two-tailed *P*-value <0.05 was considered statistically significant.

Analysis of genetic alteration

To study the genetic mutation ratios of *GSC* in different cancers, we utilized the "Gene_Mutation" module of the TIMER2 online platform. Subsequently, we investigated the characteristics of genetic alterations in *GSC* using the cBioPortal database. For this analysis, we selected the TCGA Pan Cancer Atlas Studies and Prostate Adenocarcinoma (TCGA and PanCancer Atlas) datasets. Somatic mutations and copy number alterations were obtained from UCSC Xena. In the TCGA PCa cohort, we divided the patients into two groups based on the median *GSC* expression. To examine copy number alterations in the high and low *GSC* expression groups, we used the R package "maftools."

Analysis of GSC-related genes and immune cell infiltration

To identify potential GSC-binding proteins, we evaluated the STRING database (https://string-db.org/).[22] "GSC" was queried in the "protein name" module and the key parameters were set as follows: network edges with "evidence," minimum required interaction score of "medium confidence (0.400)," and a maximum of five interactors shown in the first shell. As a result, the five available candidates were selected. Subsequently, we investigated the correlation between the mRNA expression of *GSC* and the five genes encoding GSC-binding proteins in various tumors using TIMER2. In addition, we utilized the R program to analyze *GSC*-related genes in the TCGA and DKFZ databases, focusing on the top 100 genes that showed positive or negative links with *GSC* expression. To comprehensively understand the functions of *GSC*-related genes, we conducted Gene Ontology (GO) and Kyoto Encyclopedia of Genes and Genomes (KEGG) analyses of PCa using the SangerBox portal. To explore the relationship between *GSC* expression and immune-related cells in PCa, we used the XCell portal (https://xcell.ucsf.edu).[23]

Human tissues

PCa tissues and their corresponding adjacent normal prostate tissues were obtained from the Department of Urology at Tongji Hospital, Huazhong University of Science and Technology, Wuhan, China. Fifty tissue pairs were collected for further experimental verification using real-time quanti-

tative polymerase chain reaction (RT-qPCR). After undergoing radical prostatectomy surgery, all samples were immediately stored in liquid nitrogen. Before participation, informed consent was obtained from all patients. The research protocol was approved by the Ethics Committee of Tongji Medical College, Huazhong University of Science and Technology (No. 2019CR101).

Chromatin immunoprecipitation qPCR (ChIP-qPCR)

ChIP-qPCR experiments were conducted using the ChIP assay kit (Cat#9003, Cell Signal Technology, Boston, USA). Antibodies against E2F1 (66515-1-Ig, Proteintech, Wuhan, China) and a non-specific negative control rabbit IgG (Santa Cruz, Dallas, USA) were used. Supplementary Table 1 (http://links.lww.com/CM9/B753) lists the primers specific to the *GSC* promoter.

Statistical analyses

All statistical analyses used GraphPad Prism (V. 8.0.3, San Diego, USA). The paired Student's *t*-tests were used to test *GSC* expression difference between tumor tissues and matched normal tissues. Kaplan–Meier survival analysis was used to assess the association between gene expression and the survival probability of multiple tumors. *P*-values, HRs, and 95% confidence intervals (CIs) were determined using the log-rank test. Student's *t*-tests were used to compare the mean values from two groups and gene co-expression was tested using Spearman's correlation analysis. For the functional experiments, the figure legends in the relevant figures denote the specific statistical tests used. *P*-values <0.05 were considered statistically significant.

Results

GSC is overexpressed and closely related to the prognosis in multiple tumors

To explore the role of *GSC* in the development of various tumors, we initially analyzed the expression levels of *GSC* from 33 cancer types in the TCGA dataset. Comparing the expression in tumor tissues with the corresponding adjacent tissues using TIMER2.0, we observed significant upregulation of *GSC* in multiple cancer types, including cholangiocarcinoma (CHOL), colon adenocarcinoma (COAD), esophageal carcinoma (ESCA), glioblastoma multiforme (GBM), head and neck squamous cell carcinoma (HNSC), kidney renal clear cell carcinoma (KIRC), liver hepatocellular carcinoma (LIHC), lung adenocarcinoma (LUAD), lung squamous cell carcinoma (LUSC), prostate adenocarcinoma (PRAD), rectum adenocarcinoma (READ), and uterine corpus endometrial carcinoma (UCEC). Conversely, *GSC* expression was downregulated in breast invasive carcinoma (BRCA), kidney chromophobe (KICH), and thyroid carcinoma (THCA) [Figure 1A]. To validate these findings, we expanded our analysis by including normal samples from the GTEx database, further confirming the aberrant upregulation of *GSC* in most cancer types [Figure 1B]. Further, a matched sample *t*-test between cancer and adjacent tissues revealed abnormal expression of *GSC* in several tumors, including THCA, KIRC, LUSC, BRCA, CHOL, HNSC, and LIHC [Figure 1C and Supplementary Figure 1, http://links.lww.com/CM9/B752].

Subsequently, we investigated the effect of *GSC* expression on cancer patient survival. We compared the rates of OS and PFS in patients with high or low *GSC* expression [Figure 2A,B]. Our analysis revealed that high *GSC* expression was significantly associated with worse OS in adrenocortical carcinoma (ACC) (P <0.0001, HR = 1.35), kidney renal papillary cell carcinoma (KIRP) (P = 0.037, HR = 1.23), LIHC (P = 0.017, HR = 1.07), and KIRC (P = 0.029, HR = 1.10) [Figure 2C and Supplementary Figure 2A,http://links.lww.com/CM9/B752]. In addition, PFS was significantly attenuated in the ACC (P = 0.002, HR = 1.30), PRAD (P <0.0001, HR = 1.45), KIRP (P = 0.002, HR = 1.22), cervical squamous cell carcinoma and endocervical adenocarcinoma (CESE) (P = 0.011, HR = 1.09), and KIRC (P = 0.032, HR = 1.12) patients with high *GSC* expression [Figure 2D and Supplementary Figure 2B, http://links.lww.com/CM9/B752]. Notably, the highest HR value was observed in PCa based on PFS analysis. These findings indicate that *GSC* expression is significantly upregulated in multiple cancer types and is closely associated with patient prognosis in various tumors.

GSC alterations contribute to the progression of various tumors, especially in PCa

Considering the significant impact of genetic alterations on tumor progression and the expression of protein-coding genes,[24] we analyzed five different types of *GSC* alterations (mutation, structural variant, amplification, deep deletion, and multiple alterations) using TCGA datasets through the cBioPortal. Our findings revealed that amplification was the most common alteration in LUSC (1.4%), followed by deep deletion in CHOL (2.8%), mutations in thymoma, multiple alterations in bladder urothelial carcinoma (0.2%), and structural variant in PRAD (0.2%) [Figure 3A]. Additionally, we divided the samples from the TCGA database into *GSC*-altered and unaltered groups and compared the mutation counts and tumor mutation burden between the two groups. The altered group exhibited higher mutation counts and tumor mutation burden than the unaltered group [Figure 3B]. Further, analysis of the cBioPortal database indicated that missense mutations were the most common type of *GSC* mutations in cancers [Figure 3C].

Subsequently, we divided PCa patients from the TCGA database into high and low *GSC* expression groups and analyzed gene mutations in both groups. *TP53* (17%), *SPOP* (12%), and *TTN* (12%) showed the highest mutation frequencies in the high *GSC* expression group, whereas the low *GSC* expression group showed a high frequency of mutations in *SPOP* (11%), *TTN* (8%), and *FOXA1* (6%) [Figure 3D, E]. Moreover, we compared gene expression differences between the *GSC*-altered and unaltered groups in the TCGA-PRAD cohort and intriguingly found that *GSC* was the top-ranking gene with the most significant *P*-value in the altered group [Figure 3F]. Importantly, the *GSC* expression level was significantly higher in the altered group than in the unal-

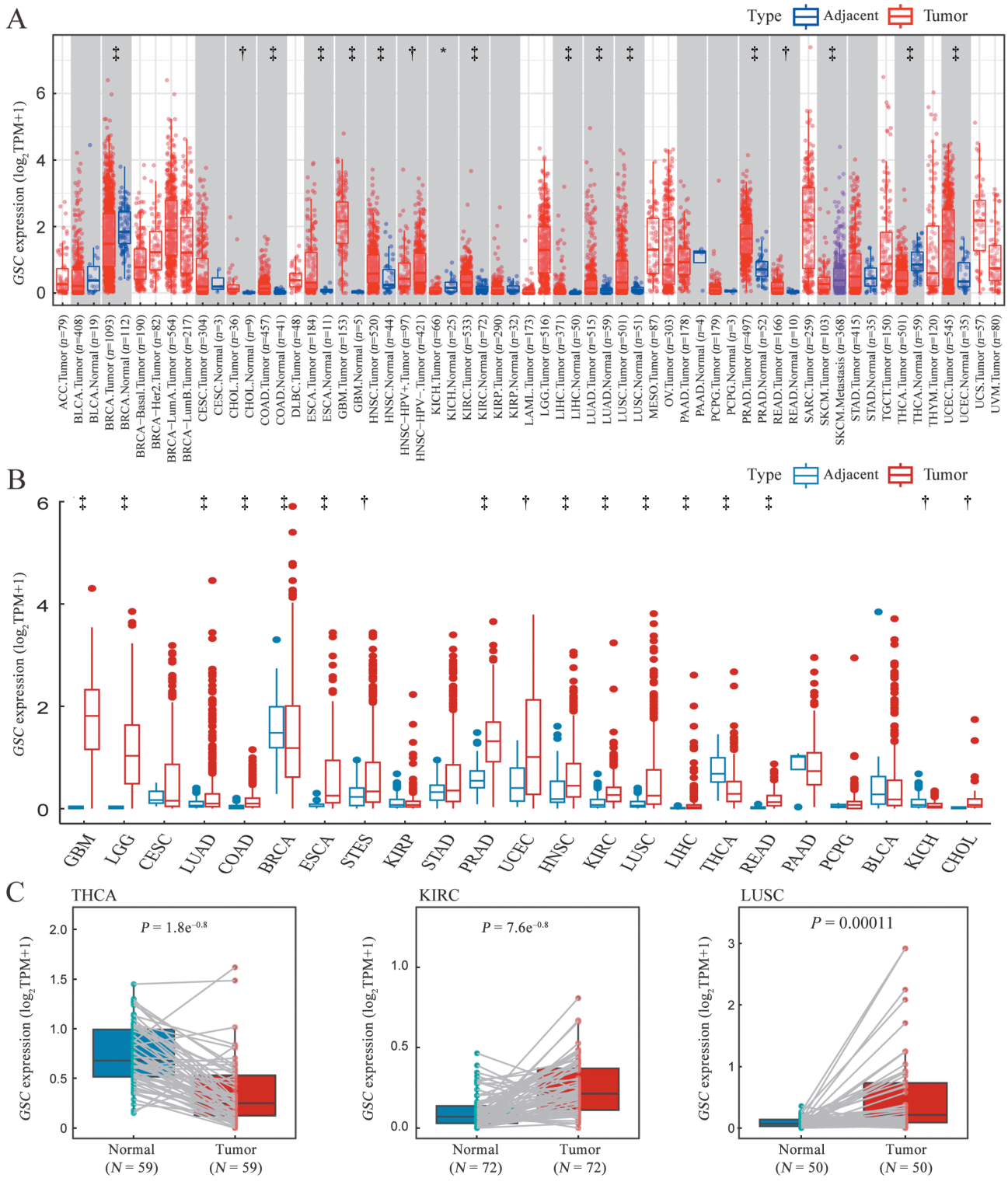

Figure 1: *GSC* expression levels in various cancers. (A) Expression levels of *GSC* in TIMER2.0 database. $^{*}P$ <0.05; $^{\dagger}P$ <0.01; $^{\ddagger}P$ <0.001. (B) *GSC* mRNA expression levels in 23 different tumor types from TCGA and GTEx database. $^{\dagger}P$ <0.01; $^{\ddagger}P$ <0.001. (C) Differential expression levels of *GSC* in tumors and corresponding normal tissues in THCA, KIRC, and LUSC. Data were presented as the median (minimum to maximum). *P*-values were calculated using a paired two-sided Student's *t*-test. BRCA: Breast invasive carcinoma; CESE: Cervical squamous cell carcinoma and endocervical adenocarcinoma; CHOL: Cholangiocarcinoma; COAD: Colon adenocarcinoma; ESCA: Esophageal carcinoma; GBM: Glioblastoma multiforme; *GSC*: Goosecoid; GTEx: Genotype-Tissue Expression; HNSC: Head and neck squamous cell carcinoma; KICH: Kidney chromophobe; KIRC: Kidney renal clear cell carcinoma; KIRP: Kidney renal papillary cell carcinoma; LIHC: Liver hepatocellular carcinoma; LUAD: Lung adenocarcinoma; LUSC: Lung squamous cell carcinoma; PRAD: Prostate adenocarcinoma; READ: Rectum adenocarcinoma; TCGA: The Cancer Genome Atlas; THCA: Thyroid carcinoma; TIMER2: Tumor Immune Estimation Resource 2.0; TPM: Transcripts per million reads; UCEC: Uterine corpus endometrial carcinoma.

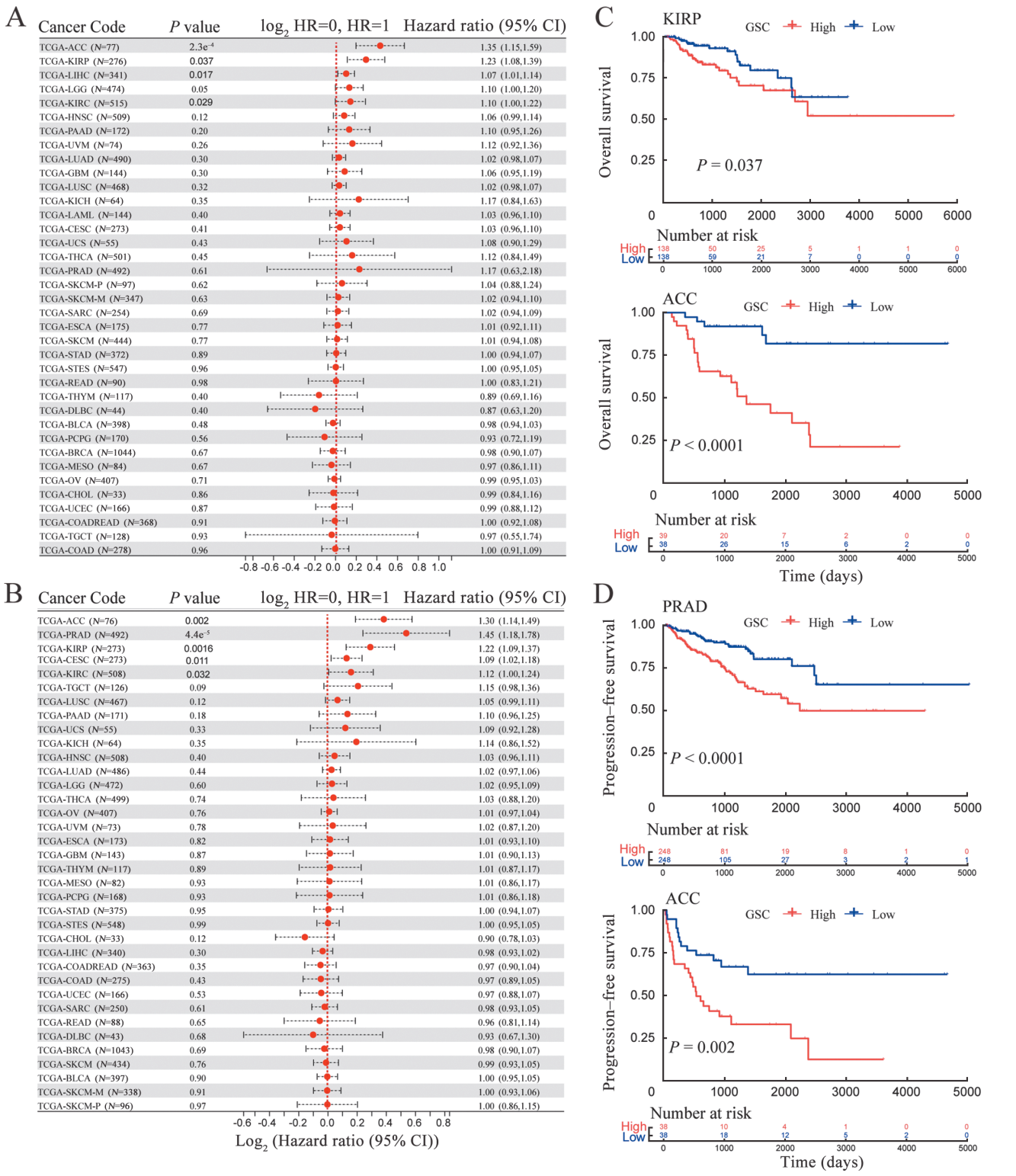

Figure 2: Prognosis value of *GSC* in tumors. (A) Forest plot of the relationship between *GSC* expression and OS in tumors. (B) Analyses of correlation between GSC expression and PFS. (C) K–M survival curves showed that patients with high *GSC* expression levels tended to have worse OS in KIRP and ACC. *P*-values were calculated using the log-rank test. (D) Kaplan–Meier survival curves showed the association between GSC expression levels and PFS in PRAD and ACC. *P*-values were calculated using the log-rank test. ACC: Adrenocortical carcinoma; CI: Confidence interval; *GSC*: Goosecoid; HR: Hazard ratio; KIRC: Kidney renal clear cell carcinoma; KIRP: Kidney renal papillary cell carcinoma; OS: Overall survival; PFS: Progression-free survival; PRAD: Prostate adenocarcinoma.

tered group [Figure 3G]. Additionally, Kaplan–Meier survival analysis revealed a poorer prognosis in patients with PCa in the altered group [Figure 3H]. Overall, *GSC* alterations were observed in multiple tumors, which were closely associated with the expression levels of *GSC* and the prognosis of patients with PCa.

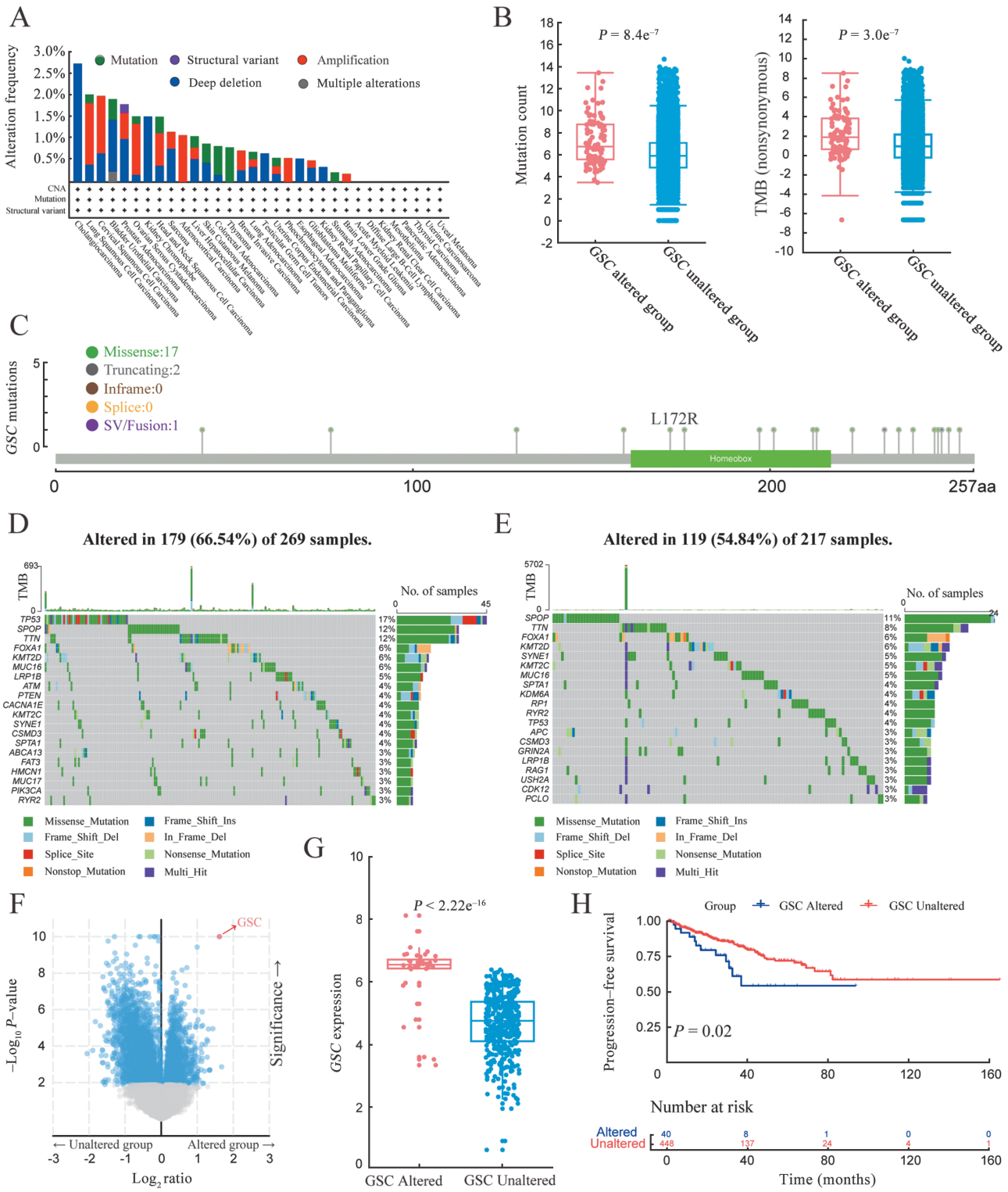

Figure 3: *GSC* alterations contribute to the progression of various tumors, especially in PCa. (A) The cBioPortal tool was used to examine *GSC* genetic alteration characteristics (mutation, structural variant, multiple alterations, amplification, and deep deletion) in 32 distinct cancers from the TCGA database. (B) Differences in mutation count and TMB between the *GSC*-altered and unaltered groups in the TCGA database. (C) The mutation sites of *GSC* in multiple tumors through the cBioPortal tool. (D,E) Detection of the top 20 genes with the highest mutation rates in the TCGA-PRAD cohort, including *GSC* high group (D) and *GSC* low group (E). (F) Differences in gene expression between *GSC*-altered and unaltered groups according to TCGA PRAD cohort. (G) The expression level of *GSC* in the mutant group was higher than that in the non-mutant group. Data were presented as the median (minimum to maximum). *P*-value was calculated using a two-sided Student's *t*-test. (H) Kaplan–Meier survival analysis showed that the altered group was related to the poorer prognosis in patients with PCa. *P*-value was calculated using the log-rank test. *GSC*: Goosecoid; PCa: Prostate cancer; PRAD: Prostate adenocarcinoma; TCGA: The Cancer Genome Atlas; TMB: Tumor mutation burden.

GSC is highly associated with PCa clinical characteristics and potentiates PCa progression in vitro and in vivo

In PCa, we observed a significant overexpression of *GSC* in tumor tissues compared with their corresponding normal tissues in multiple independent datasets, including TCGA [Figure 4A], GEO (GSE 46602, Figure 4B), and our own PCa tissues [Figure 4C]. To investigate the clinical implications of *GSC* expression in PCa, we examined its potential correlation with clinical characteristics using three independent datasets: TCGA, DKFZ, and our PCa tissues. These findings demonstrated that patients with PCa with a high Gleason score had significantly higher *GSC* expression [Figure 4D,G and Supplementary Figure 3A, http://links.lww.com/CM9/B752]. Moreover, a robust correlation was observed between the advanced tumor stage and high *GSC* expression [Figure 4E,H and Supplementary Figure 3B, http://links.lww.com/CM9/B752]. High *GSC* expression was also strongly associated with lymph node metastasis [Figure 4F] and elevated prostate-specific antigen (PSA) levels [Figure 4I] in TCGA and our own PCa cohorts, respectively. These findings indicated a close relationship between *GSC* and PCa progression. Consistent with these findings, higher *GSC* expression levels were also associated with an increased risk of BCR in patients with PCa [Figure 4J–L], and receiver operating characteristic (ROC) analysis revealed that *GSC* expression levels could serve as a reliable prognostic indicator for patients with PCa [Supplementary Figure 3C, D, http://links.lww.com/CM9/B752].

Having revealed the prognostic role of *GSC* in patients with PCa, we investigated its functional effects. Our experimental studies utilized specific *GSC*-targeting

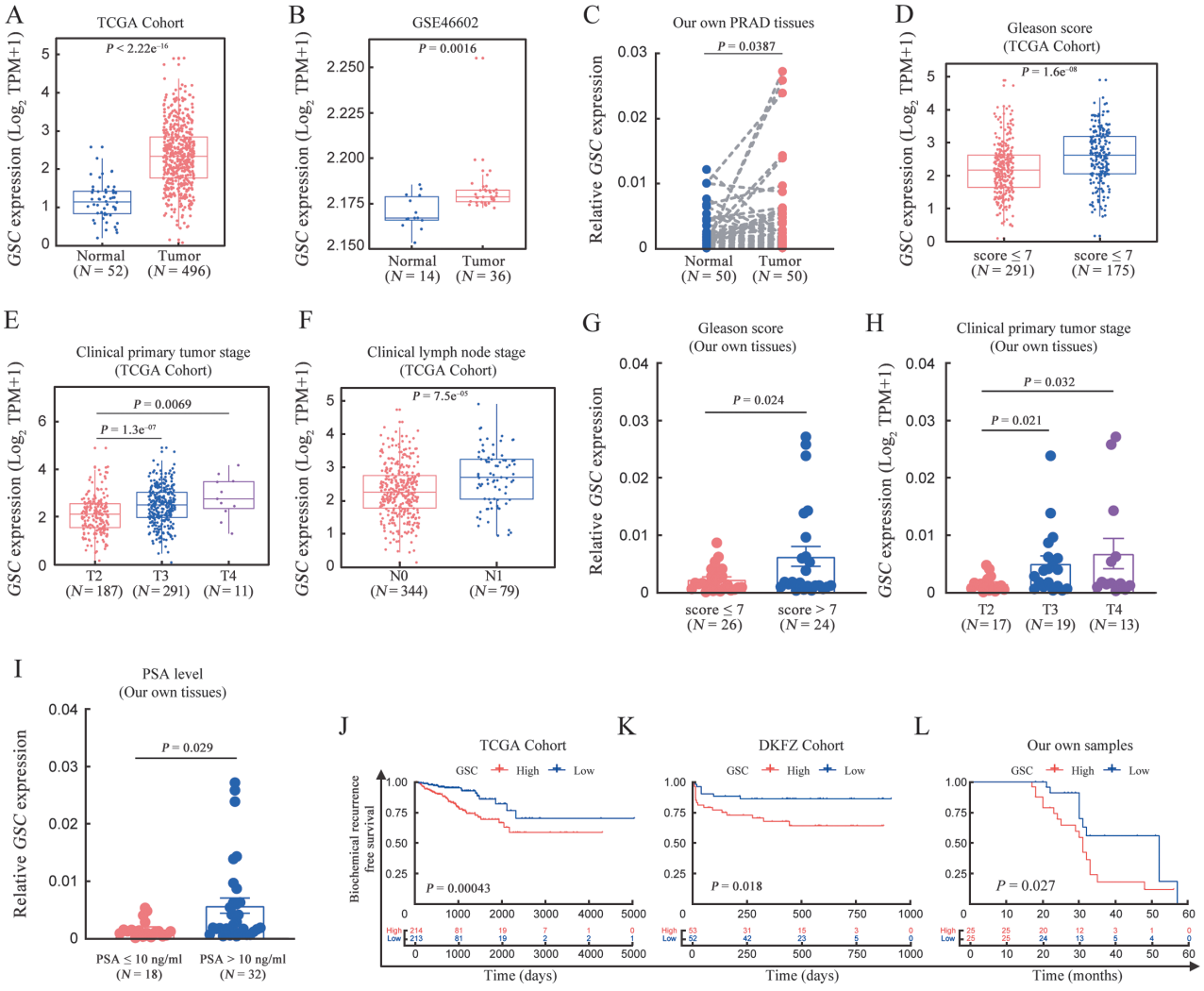

Figure 4: Clinical characteristics of *GSC* in PCa. (A–C) *GSC* was significantly overexpressed in prostate tumor tissues compared with normal tissues from multiple independent databases, including the TCGA cohort, GEO (GSE46602) cohort, and our PCa tissues. Data are presented as the median (minimum to maximum). *P*-values were calculated using a two-sided Student's *t*-test in TCGA and GEO PCa samples, whereas it was calculated using a paired two-sided Student's *t*-test in our PCa tissues. (D–F) Elevated *GSC* expression correlated with higher Gleason score, advanced primary tumor stage, and lymph node metastasis in the TCGA cohort. *P*-values were determined by the two-sided Student's *t*-test. (G–I) High *GSC* expression correlated with higher Gleason score, advanced primary tumor stages, and elevated PSA level in our PCa samples. *P*-values were determined by the two-sided Student's *t*-test. (J–L) Kaplan–Meier plots suggested increased BCR risks of PCa patients with tumors expressing higher *GSC* levels in three independent cohorts. BCR: Biochemical recurrence; *GSC*: Goosecoid; PCa: Prostate cancer; PRAD: Prostate adenocarcinoma; PSA: Prostate-specific antigen; TCGA: The Cancer Genome Atlas.

small hairpin RNAs (shRNAs) to achieve a stable knockdown of *GSC* expression in C4-2 and 22Rv1 PCa cells. The efficacy of the knockdown was confirmed using RT-qPCR and Western blotting [Figure 5A, B]. To further explore the potential impact of *GSC* on PCa, we conducted CCK-8, colony formation, and transwell assays to assess cell proliferation and migration abilities *in vitro* [Figure 5C–E]. These results demonstrated that *GSC* knockdown significantly suppressed the proliferation and migration of C4-2 and 22Rv1 cells *in vitro*. To evaluate the effect of *GSC in vivo*, we subcutaneously injected *GSC*-knockdown C4-2 and 22Rv1 cells into nude mice. Interestingly, the results revealed that *GSC* knockdown significantly inhibited the growth rate of xenograft tumors [Figure 5F]. The tumor weight in the *GSC* knockdown group was significantly lower compared to the control group [Figure 5G], consistent with the *in vitro* findings. These findings highlight the oncogenic effects of *GSC* on PCa *in vitro* and *in vivo*.

Transcription factor E2F1 drives the expression of GSC in PCa

To further investigate the potential tumorigenic mechanisms of *GSC*, STRING database analysis was implemented to identify *GSC*-binding proteins. Consequently, five *GSC*-binding proteins were selected: *E2F1*, *E2F2*, *E2F3*, *SPI1*, and *RB1*. The protein–protein interaction networks of these proteins are shown in Figure 6A. We analyzed the correlation between *GSC* and these five genes in 33 cancer types using the GEPIA2 database [Figure 6B]. The results indicated a strong correlation between these genes and *GSC* in multiple tumor types, including PCa. Additionally, we performed gene set enrichment analysis (GSEA) analysis to explore potential pathways associated with *GSC* in PCa. Interestingly, we discovered that *GSC* was likely a target of the E2F family [Supplementary Figure 4A,B, http://links.lww.com/CM9/B752], which is known to facilitate PCa development by activating downstream genes.[25] Therefore, we hypothesized that *GSC* was a downstream target of the E2F family in PCa.

Subsequently, we analyzed the correlation between *GSC* and E2F transcription factors (*E2F1*, *E2F2*, and *E2F3*) using TCGA, DKFZ, and our own sample data. In the TCGA and DKFZ cohorts, we observed a positive correlation between the expression of *E2F1* and *GSC*, with the correlation coefficient (R) value of *E2F1* being more significant than that of *E2F2* and *E2F3* in both datasets [Figure 6C, D and Supplementary Figure 4C, D, http://links.lww.com/CM9/B752]. Consistently, we found a remarkable positive correlation between the expression of *GSC* and *E2F1* in our own PCa tissue samples [Figure 6E]. Further, we stably knocked down the expression of *E2F1* in C4-2 and 22Rv1 cells using two independent shRNAs. RT-qPCR and Western blotting experiments revealed a significant attenuation of *GSC* expression after *E2F1* suppression in PCa cells [Figure 6F, G]. Importantly, analysis of publicly available ChIP-seq data from LNCaP cells[26] demonstrated a high enrichment of E2F1 ChIP-seq signals in the *GSC* promoter region [Figure 6H], which was further validated by ChIP-qPCR in C4-2 and 22Rv1 cells [Figure 6I]. In summary, these results suggest that the transcription factor *E2F1* facilitates *GSC* expression in PCa.

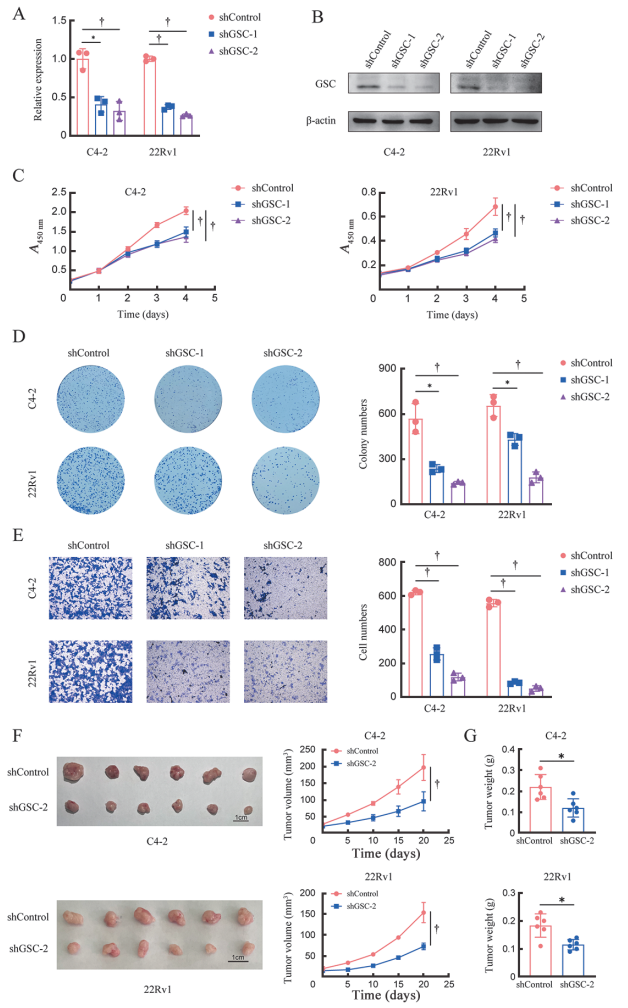

Figure 5: The oncogenic functions of *GSC* in PCa. (A) RT-qPCR indicated the *GSC* transcript levels (normalized to GAPDH) in C4-2 and 22Rv1 cells transfected with shControl or sh*GSC* plasmids. Data were shown as the mean ± SD. $^{*}P$ <0.01; $^{\dagger}P$ <0.001 were calculated using a two-sided Student's *t*-test. (B) Western blotting indicated the *GSC* expression levels in C4-2 and 22Rv1 cells transfected with shControl or shGSC plasmids. (C) CCK-8 assays illustrated the change of cell viability in C4-2 and 22Rv1 cells stably transfected with shControl or sh*GSC*. Data were shown as the mean ± SEM with five replicates. $^{\dagger}P$ <0.001 compared with control by the two-sided Student's *t*-test. (D) Colony formation assays showed the proliferation of C4-2 and 22Rv1 cells stably transfected with shControl or shGSC. Data were shown as the mean ± SD. $^{*}P$ <0.01; $^{\dagger}P$ <0.001 compared with shControl by the two-sided Student's *t*-test. (E) Transwell migration assays demonstrated the migration ability of C4-2 and 22Rv1 cells stably transfected with shControl or shGSC. Data were shown as the mean ± SD. $^{\dagger}P$ <0.001 compared with shControl by a two-sided Student's *t*-test. (F) Representative images and growth curves of xenograft tumors derived from C4-2 and 22Rv1 cells with *GSC* suppression in nude mice. Data were shown as the mean ± SEM for six mice per group. $^{\dagger}P$ <0.001 compared with shControl by the two-sided Student's *t*-test. (G) The weight of xenograft tumors derived from C4-2 and 22Rv1 cells with *GSC* suppression in nude mice. The results were shown as the mean ± SD for six mice per group. $^{\dagger}P$ <0.01 compared with shControl by a two-sided Student's *t*-test. CCK-8: Cell Counting Kit-8; GAPDH: Glyceraldehyde-3-phosphate dehydrogenase; *GSC*: Goosecoid; PCa: Prostate cancer; RT-qPCR: Real-time quantitative polymerase chain reaction; SD: Standard deviation; SEM: Standard error of the mean; sh: Small harpin.

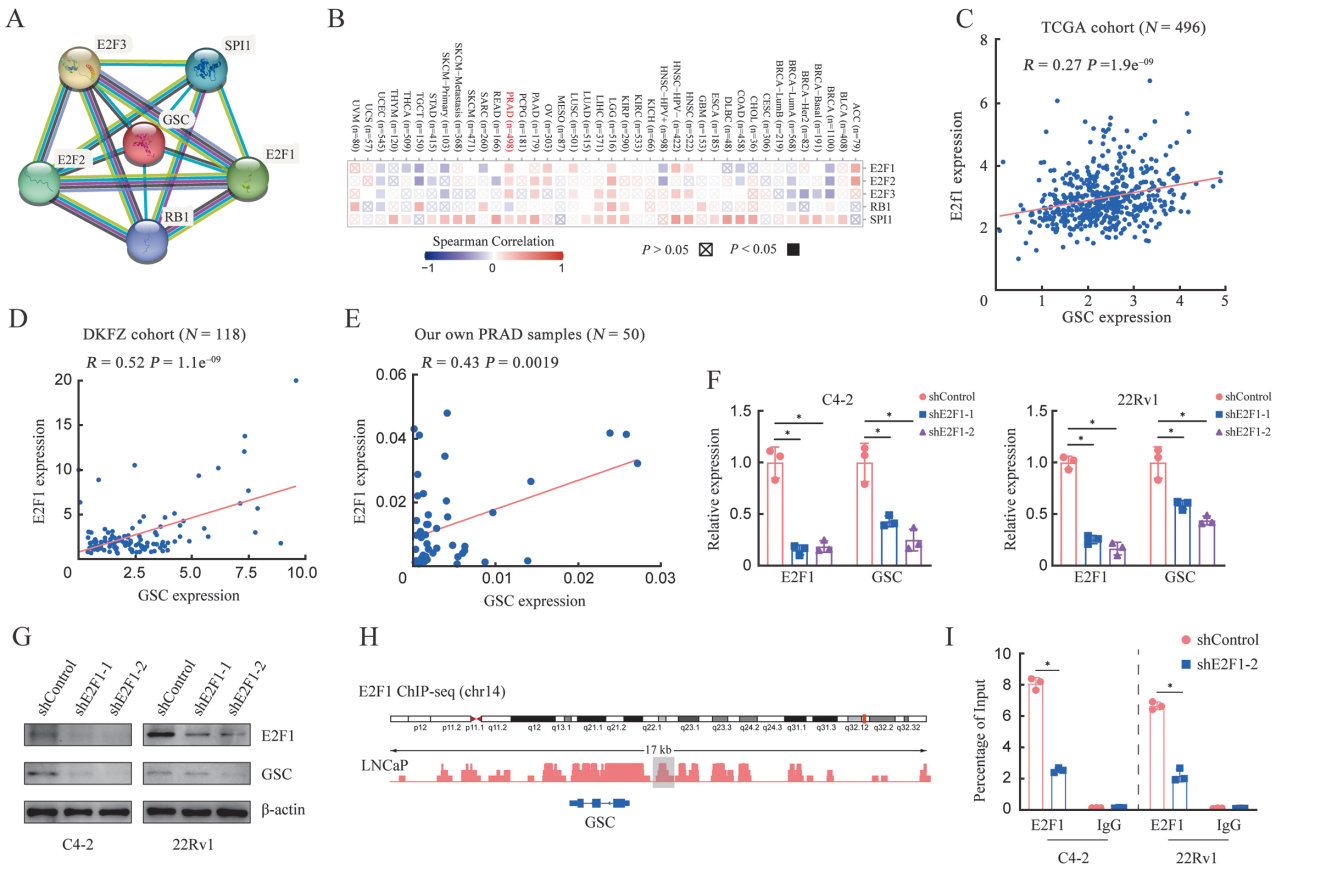

Figure 6: Transcription factor *E2F1* drives *GSC* expression in PCa. (A) The potential *GSC*-binding proteins were illustrated using the STRING tool (*E2F1*, *E2F2*, *E2F3*, *SPI1*, and *RB1*). (B) The corresponding heatmap data of *GSC* and its potential binding proteins in multiple tumors using the TIMER2.0 tool. (C–E) The expression correlations of *GSC* with *E2F1* were measured in the TCGA cohort, DKFZ cohort, and our patient samples with PCa. All *P*-values and *R*-values were calculated using the Spearman correlation analysis. (F) Real-time qPCR indicated the *E2F1* and *GSC* transcript levels (normalized to GAPDH) in C4-2 and 22Rv1 cells transfected with shControl or sh*E2F1* plasmids. (G) Western blotting indicated the *GSC* and *E2F1* expression levels in C4-2 and 22Rv1 cells transfected with shControl or sh*E2F1* plasmids. (H) Epigenetic track, obtained from publicly available *E2F1* ChIP-seq data in LNCaP cells, revealed the enrichment of ChIP-seq signals at the *GSC* promoter region. (I) ChIP-qPCR results showed the significant recruitment of *E2F1* at the *GSC* promoter region, and *E2F1* recruitment attenuated after silencing *E2F1* in C4-2 and 22Rv1 cells. Data were shown as the mean ± SD. $^{*}P$ <0.001 was calculated using the two-sided Student's *t*-test. ACC: Adrenocortical cancer; BLCA: Bladder urothelial carcinoma; BRCA: Breast invasive carcinoma; ChIP-qPCR: Chromatin immunoprecipitation qPCR; CESC: Cervical and endocervical cancer; CHOL: Cholangiocarcinoma; COAD: Colon adenocarcinoma; DLBC: Diffuse Large B-cell Lymphoma; *E2F1*: E2F transcription factor 1; ESCA: Esophageal carcinoma; GBM: Glioblastoma multiforme; *GSC*: Goosecoid; HNSC: Head and Neck squamous cell carcinoma; KICH: Kidney Chromophobe; KIRC: Kidney renal clear cell carcinoma; KIRP: Kidney renal papillary cell carcinoma; IgG: Immunoglobulin G; LGG: Lower Grade Glioma; LIHC: Liver hepatocellular carcinoma; LUAD: Lung adenocarcinoma; LUSC: Lung squamous cell carcinoma; MESO: Mesothelioma; OV: Ovarian serous cystadenocarcinoma; PAAD: Pancreatic adenocarcinoma; PCa: Prostate cancer; PCPG: Pheochromocytoma and Paraganglioma; PRAD: Prostate adenocarcinoma; READ: Rectum adenocarcinoma; SARC: Sarcomav; SD: Standard deviation; SKCM: Skin Cutaneous Melanoma; sh: Small harpin; STAD: Stomach adenocarcinoma; TCGA: The Cancer Genome Atlas; TIMER2: Tumor Immune Estimation Resource 2.0; TGCT: Testicular Germ Cell Tumors; THCA: Thyroid carcinoma; THYM: Thymoma; UCEC: Uterine Corpus Endometrial Carcinoma; UCS: Uterine Carcinosarcoma; UVM: Uveal Melanoma.

GSC participates in regulating immune signaling and metabolism in PCa

To investigate the potential biological functions of *GSC* in PCa, we performed GO and KEGG enrichment analysis on the top 200 genes correlated with *GSC* in PCa. The enrichment distribution of *GSC*-related genes in the TCGA and DKFZ cohorts is illustrated in Figure 7A,B, respectively. Moreover, KEGG analysis indicated that *GSC* might regulate the erythroblastic oncogene B (ErbB) signaling pathway, retinol metabolism, metabolic pathway, and T cell receptor signaling pathway in the TCGA and DKFZ databases. Additionally, *GSC* might also be involved in the B cell receptor signaling pathway, T helper cell (Th)1 and Th2 cell differentiation, and IL-17 signaling pathway in the TCGA and DKFZ databases, respectively [Figure 7C,D]. These results suggest that *GSC* and related genes might be involved in metabolism and immune signaling regulation. Further, GO analysis results indicated that the mitogen-activated protein kinase (MAPK) cascade pathway was enriched in both TCGA and DKFZ databases [Figure 7E,F]. Consistently, GSEA analysis also demonstrated that *GSC* was closely associated with the regulation of MAPK cascade in PCa [Figure 7G,H].

Given that the above results suggest a potential role for *GSC* in regulating the tumor microenvironment (TME), which affects PCa progression,[27] we further explored the potential connection between *GSC* and immune cell infiltration in PCa. We examined variations in immune cell infiltration between groups with high and low *GSC*

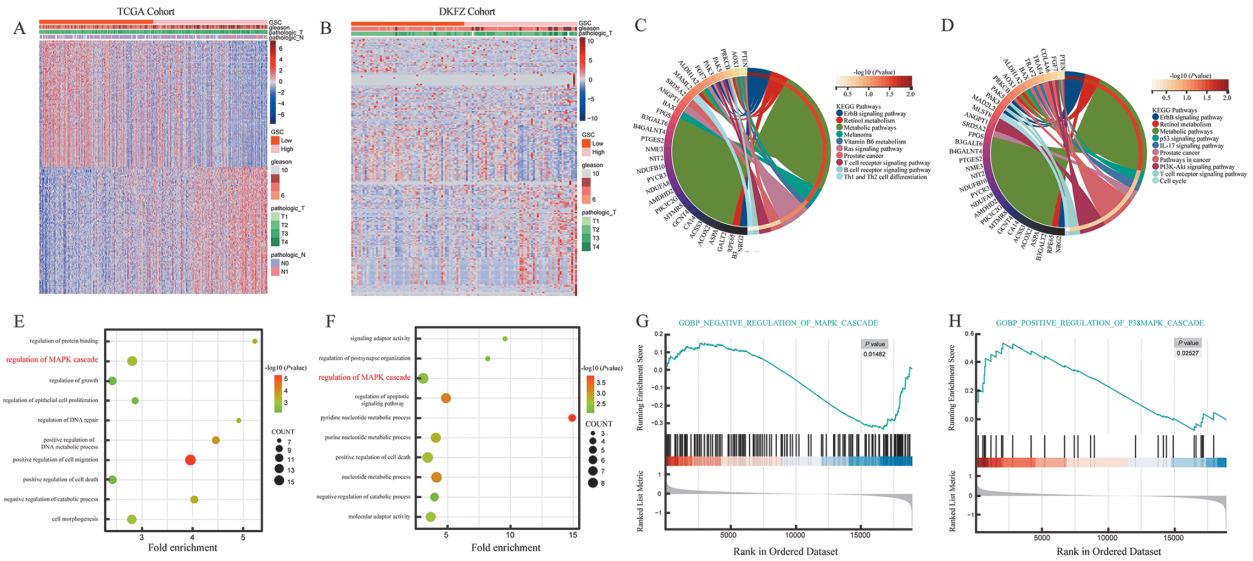

Figure 7: *GSC*-related genes enrichment analysis in PCa by TCGA and DKFZ databases. (A,B) Heatmap illustrated the enrichment patterns of the top 200 genes positively (100) or negatively (100) correlated with *GSC* expression of PCa in the TCGA and DKFZ databases. (C,D) KEGG pathway enrichment analyses were applied to the 200 GSC-related genes in the TCGA and DKFZ cohorts. (E,F) The top 200 *GSC*-related genes in the TCGA and DKFZ cohorts were used in GO pathway enrichment studies. (G,H) GSEA analyses showed that *GSC* was related to the regulation of MAPK cascade in PCa. *E2F1*: E2F transcription factor 1; *GSC*: Goosecoid; MAPK: Mitogen-activated protein kinase; PCa: Prostate cancer; TCGA: The Cancer Genome Atlas.

expression levels. Interestingly, high *GSC* expression levels were associated with increased endothelial and mesenchymal stem cell infiltration, whereas low *GSC* expression levels were possibly linked to enhanced B cell and myocyte infiltration [Supplementary Figure 5A, B, http://links.lww.com/CM9/B752]. Additionally, in the TCGA cohort, the high *GSC* expression group showed significantly higher levels of CD8+ T cells, Th1 and Th2, and macrophage expression, while the low *GSC* expression group had higher a regulatory T cells level [Supplementary Figure 5A, http://links.lww.com/CM9/B752]. There was no significant difference in natural killer cell between the high and low *GSC* expression groups. In contrast, in the DKFZ cohort, there were no significant changes in the expression of these immune cells between the two groups [Supplementary Figure 5B, http://links.lww.com/CM9/B752], which may be attributed to the limited sample size of the DKFZ cohort. Taken together, these findings suggest that *GSC* plays a regulatory role in immune cell infiltration within the tumor microenvironment of PCa.

Inhibiting GSC enhances the therapeutic effects of trametinib in PCa

To gain a better understanding of the impact of *GSC* on drug responses in cancer, we analyzed 481 small molecules from the Cancer Therapeutics Response Portal (CTRP) database and examined the correlation between *GSC* expression level and the drug IC50 [Supplementary Table 2, http://links.lww.com/CM9/B754]. Interestingly, we found that trametinib ($R = 0.24$, FDR = 0.000124) showed the strongest positive correlation with *GSC* [Figure 8A]. Previous studies have reported the potential application of trametinib in PCa treatment.[28,29] Based on these findings, we further investigated whether the therapeutic effects of trametinib were influenced by *GSC* expression in PCa. Notably, CCK-8 and colony formation assays revealed that trametinib (2 μmol/L, following a previous study[29]) moderately suppressed the growth of PCa cells. However, a significantly stronger inhibitory effect on the proliferation of C4-2 and 22Rv1 cells was observed when *GSC* expression levels were significantly reduced [Figure 8B–E]. These results suggest that the inhibition of *GSC* expression could enhance the therapeutic effects of trametinib, thereby indicating the potential of combining trametinib with *GSC*-targeting drugs as a novel therapeutic strategy for PCa.

Discussion

In this study, our findings revealed a significant upregulation of *GSC* mRNA expression in various malignancies, including PCa. Further, a comprehensive prognostic analysis demonstrated that high *GSC* expression was associated with worse survival outcomes in multiple cancer types. Specifically, in PCa, patients with high *GSC* expression exhibited poor progression-free and BCR survival. Moreover, the upregulation of *GSC* in patients with PCa consistently correlated with higher Gleason scores, advanced tumor stages, lymph node metastasis, and elevated PSA levels. These findings strongly support using *GSC* as an independent PCa diagnosis and prognosis marker. To further elucidate its functional role, detailed *in vitro* and *in vivo* experiments were conducted, which demonstrated that *GSC* could promote the proliferation and migration of PCa cells. Additionally, we reported, pioneeringly, a potential mechanism underlying *GSC* overexpression, whereby the transcription factor *E2F1* bound to the *GSC* promoter region in PCa, which was confidently validated through ChIP-qPCR experiments. Moreover, our study revealed that altera-

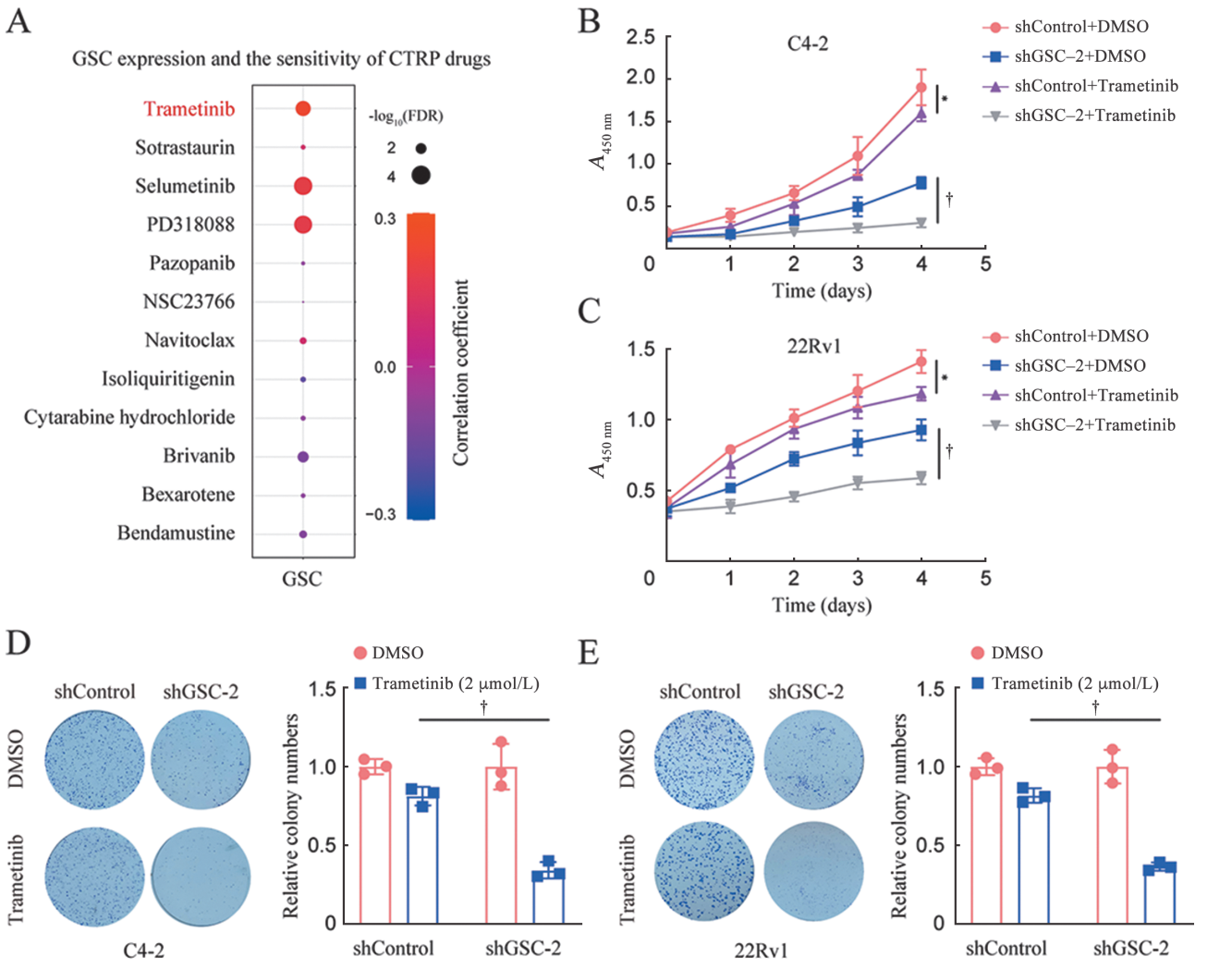

Figure 8: Inhibiting *GSC* enhances the therapeutic effects of trametinib in PCa. (A) Bubble diagram showed the correlation between *GSC* expression and small molecules from the CTRP database. FDR and correlation coefficients were calculated using Spearman correlation analysis. (B, C) C4-2 and 22Rv1 cells stably transfected with shControl or sh*GSC*-2 plasmids were treated with dimethyl sulfoxide (DMSO) or trametinib (2 μmol/L) and then subjected to CCK-8 cell proliferation assay. Data were shown as the mean ± SEM with five replicates. (D,E) C4-2 and 22Rv1 cells stably transfected with shControl or shGSC-2 plasmids were seeded in 6-well plates and incubated for 2 weeks. Cells were treated with DMSO or trametinib (2 μmol/L). Data were shown as the mean ± SD. $^{*}P$ <0.01; $^{\dagger}P$ <0.001 compared with control using the two-sided Student's *t*-test. CTRP: The Cancer Therapeutics Response Portal; CCK-8: Cell Counting Kit-8; DMSO: Dimethyl sulfoxide; FDR: False discovery rate; GO: Gene Ontology; *GSC*: Goosecoid; KEGG: Kyoto Encyclopedia of Genes and Genomes; PCa: Prostate cancer; SD: Standard deviation; SEM: Standard error of the mean; sh: Small harpin.

tions in *GSC* expression levels could influence the response of PCa cells to trametinib, highlighting the potential therapeutic value of targeting *GSC* in PCa.

GSC, a protein containing homeoboxes, was initially identified as a transcriptional repressor involved in the regulation of vertebrate embryo development.[30] In the context of malignant diseases, *GSC* had been implicated in the development and metastasis of several tumors. For instance, Kang *et al*[13] reported a significant association between elevated *GSC* expression, lymph node metastasis, and poor prognosis in ovarian serous carcinomas. Additionally, Hartwell *et al*[9] revealed that aberrant *GSC* expression enhanced the ability of breast cancer cells to develop pulmonary metastasis. Similarly, Xue *et al*[14] demonstrated that *GSC* overexpression promoted the migration and invasion of hepatocellular carcinoma cells through epithelial–mesenchymal transition *in vitro*. However, there remains a gap in our understanding of the comprehensive functional role of *GSC* in pan-cancer, particularly in PCa. Therefore, in this study, we systematically explored the functional involvement of *GSC* in various malignancies, with a specific focus on PCa. Our analysis encompassed differential expression, prognostic impact, genetic alterations, immune cell infiltration, and drug responses associated with *GSC*. Importantly, we experimentally investigated the effects of *GSC* on PCa cell proliferation, migration, and drug response, providing experimental evidence to support our previous bioinformatic analysis.

Accumulating evidence suggests that genetic alterations play a crucial role in driving the progression of normal cells from the hyperplastic and dysplastic stages to metastatic disease, including invasive cancer.[31,32] Therefore, the analysis of gene alterations is essential for gaining novel insights into the role of oncogenes in cancer development.[33] In line with this, we investigated the muta-

tion types of *GSC* across various cancers and observed that missense mutations were the most frequently occurring mutation type in multiple cancer types. Further, in patients with PCa from the TCGA cohort, *GSC* ranked as the top gene with the most significant *P*-value in the *GSC* alteration group. Notably, we discovered a strong association between genetic alterations in *GSC* and poorer PFS in patients with PCa, indicating its involvement in PCa progression and highlighting its potential as an attractive target for PCa diagnosis and prognosis.

The E2F family consists of eight transcription factors that encode 10 proteins, which play critical roles in various biological processes such as genomic integrity, cell cycle development, differentiation, metabolism, and apoptosis.[34,35] These transcription factors are highly abundant in cancer and have been implicated as inducers of several human carcinomas, including breast, colon, oral, and PCa.[36] Among the E2F family, *E2F1* is particularly essential for the development of PCa. For instance, Song *et al*[37] discovered that *E2F1* may promote the neuroendocrine trans-differentiation of PCa by facilitating the expression of *RACGAP1* and maintaining *EZH2* expression levels through the ubiquitin-proteasome pathway. Additionally, Mandigo *et al*[38] demonstrated that the cooperation between AR and *E2F1* elicited novel transcriptional networks that promoted cancer malignant phenotypes, especially those related to evading cell death in PCa. However, despite being a conserved transcription factor, the upstream regulatory mechanisms of *GSC* remained unclear. Interestingly, we discovered a positive correlation between the expression of *E2F1* and *GSC* based on public databases and our tissue samples. Mechanistically, we performed ChIP-qPCR to validate whether *E2F1* induced *GSC* expression by binding to its promoter.

To date, androgen deprivation therapy remains the most commonly used therapeutic approach for PCa, while targeted drug therapy has not been widely adopted to manage this disease.[39,40] Trametinib, primarily employed in treating melanoma and non-small cell lung cancer with specific genetic mutations,[41,42] is a targeted therapeutic drug for cancer treatment. Its primary mechanism of action is the suppression of mitogen-activated kinase (MEK) proteins, which are involved in the MAPK pathway.[43] By inhibiting MEK activity, trametinib can effectively impede the growth of cancer cells that rely on the MAPK pathway for survival. This property contributes to tumor shrinkage and improves patient outcomes.[44] Several studies have suggested trametinib as a potential candidate for the treatment of PCa. For example, Ciccarelli *et al*[28] found that trametinib successfully inhibited the growth of PCa cells *in vitro*. Further, a study by Li *et al*[29] strongly supported the utility of the MEK inhibitor trametinib for the treatment of enzalutamide-resistant PCa, and the combination of trametinib with enzalutamide was highly effective in managing castration-resistant PCa. However, the effect of trametinib on PCa treatment remained largely unknown. In this study, we provided novel insight into the therapeutic effect of trametinib in PCa. We demonstrated that the response of PCa cells to trametinib could be influenced by *GSC*, which was closely associated with MAPK pathway activation. These findings suggested that combining trametinib with drugs targeting *GSC* represents a promising and novel therapeutic strategy for PCa.

In conclusion, our study revealed that *GSC* was dysregulated and significantly associated with the prognosis of patients with PCa. We systematically investigated the functional significance of alterations in *GSC* expression in PCa, including their impact on prognosis, genetic alterations, immune cell infiltration, and drug response. Further, detailed experiments confirmed that *GSC* was regulated by the transcription factor *E2F1* and functioned as an oncogene in PCa. Importantly, we demonstrated that suppression of *GSC* expression enhanced the therapeutic effects of trametinib in PCa. Taken together, our findings suggest that *GSC* can serve as an independent biomarker for PCa prognosis and as a potential target for therapeutic interventions.

Funding

This study was supported by the National Natural Science Foundation of China (Nos. 82173068, 81974400) and the Applied Basic Research Plan from Qinghai Provincial Department of Science and Technology (No. 2021-ZJ-723).

Conflicts of interest

None.

Data availability

Data used in this study are available from the corresponding author on reasonable request. The experimental details are available in the Supplementary Methods, http://links.lww.com/CM9/B753.

References

1. Sung H, Ferlay J, Siegel RL, Laversanne M, Soerjomataram I, Jemal A, *et al*. Global cancer statistics 2020: GLOBOCAN estimates of incidence and mortality worldwide for 36 cancers in 185 countries. CA Cancer J Clin 2021;71:209–249. doi: 10.3322/caac.21660.
2. Xia C, Dong X, Li H, Cao M, Sun D, He S, *et al*. Cancer statistics in China and United States, 2022: Profiles, trends, and determinants. Chin Med J 2022;135:584–590. doi: 10.1097/CM9.0000000000002108.
3. Cha HR, Lee JH, Ponnazhagan S. Revisiting immunotherapy: A focus on prostate cancer. Cancer Res 2020;80:1615–1623. doi: 10.1158/0008-5472.CAN-19-2948.
4. Bergengren O, Pekala KR, Matsoukas K, Fainberg J, Mungovan SF, Bratt O, *et al*. 2022 update on prostate cancer epidemiology and risk factors-a systematic review. Eur Urol 2023;84:191–206. doi: 10.1016/j.eururo.2023.04.021.
5. Jin K, Qiu S, Chen B, Zhang Z, Zhang C, Zhou X, *et al*. DOK3 promotes proliferation and inhibits apoptosis of prostate cancer via the NF-κB signaling pathway. Chin Med J 2023;136:423–432. doi: 10.1097/CM9.0000000000002251.
6. Gao P, Xia JH, Sipeky C, Dong XM, Zhang Q, Yang Y, *et al*. Biology and clinical implications of the 19q13 aggressive prostate cancer susceptibility locus. Cell 2018;174:576–589. e18. doi: 10.1016/j.cell.2018.06.003.
7. Ding Y, Li N, Dong B, Guo W, Wei H, Chen Q, *et al*. Chromatin remodeling ATPase BRG1 and PTEN are synthetic lethal in prostate cancer. J Clin Invest 2019;129:759–773. doi: 10.1172/JCI123557.

8. Tsujino T, Takai T, Hinohara K, Gui F, Tsutsumi T, Bai X, *et al*. CRISPR screens reveal genetic determinants of PARP inhibitor sensitivity and resistance in prostate cancer. Nat Commun 2023;14:252. doi: 10.1038/s41467-023-35880-y.
9. Hartwell KA, Muir B, Reinhardt F, Carpenter AE, Sgroi DC, Weinberg RA. The Spemann organizer gene, Goosecoid, promotes tumor metastasis. Proc Natl Acad Sci U S A 2006;103:18969–18974. doi: 10.1073/pnas.0608636103.
10. Yasuo H, Lemaire P. Role of Goosecoid, Xnot and Wnt antagonists in the maintenance of the notochord genetic programme in Xenopus gastrulae. Development 2001;128:3783–3793. doi: 10.1242/dev.128.19.3783.
11. Luu O, Nagel M, Wacker S, Lemaire P, Winklbauer R. Control of gastrula cell motility by the Goosecoid/Mix.1/ Siamois network: Basic patterns and paradoxical effects. Dev Dyn 2008;237:1307–1320. doi: 10.1002/dvdy.21522.
12. Clouthier DE, Hosoda K, Richardson JA, Williams SC, Yanagisawa H, Kuwaki T, *et al*. Cranial and cardiac neural crest defects in endothelin-A receptor-deficient mice. Development 1998;125:813–824. doi: 10.1242/dev.125.5.813.
13. Kang KW, Lee MJ, Song JA, Jeong JY, Kim YK, Lee C, *et al*. Overexpression of goosecoid homeobox is associated with chemoresistance and poor prognosis in ovarian carcinoma. Oncol Rep 2014;32:189–198. doi: 10.3892/or.2014.3203.
14. Xue TC, Ge NL, Zhang L, Cui JF, Chen RX, You Y, *et al*. Goosecoid promotes the metastasis of hepatocellular carcinoma by modulating the epithelial-mesenchymal transition. PLoS One 2014;9:e109695. doi: 10.1371/journal.pone.0109695.
15. Watabe T, Kim S, Candia A, Rothbächer U, Hashimoto C, Inoue K, *et al*. Molecular mechanisms of Spemann's organizer formation: Conserved growth factor synergy between Xenopus and mouse. Genes Dev 1995;9:3038–3050. doi: 10.1101/gad.9.24.3038.
16. Moon RT, Kimelman D. From cortical rotation to organizer gene expression: Toward a molecular explanation of axis specification in Xenopus. Bioessays 1998;20:536–545. doi: 10.1002/(SICI)1521-1878(199807)20:7<536::AID-BIES4>3.0.CO;2-I.
17. Ju X, Casimiro MC, Gormley M, Meng H, Jiao X, Katiyar S, *et al*. Identification of a Cyclin D1 network in prostate cancer that antagonizes epithelial–mesenchymal restraint. Cancer Res 2014;74:508–519. doi: 10.1158/0008-5472.CAN-13-1313.
18. Camoriano M, Kinney SR, Moser MT, Foster BA, Mohler JL, Trump DL, *et al*. Phenotype-specific CpG island methylation events in a murine model of prostate cancer. Cancer Res 2008;68:4173–4182. doi: 10.1158/0008-5472.CAN-07-6715.
19. Li T, Fu J, Zeng Z, Cohen D, Li J, Chen Q, *et al*. TIMER2.0 for analysis of tumor-infiltrating immune cells. Nucleic Acids Res 2020;48:W509–W514. doi: 10.1093/nar/gkaa407.
20. Gao J, Aksoy BA, Dogrusoz U, Dresdner G, Gross B, Sumer SO, *et al*. Integrative analysis of complex cancer genomics and clinical profiles using the cBioPortal. Sci Signal 2013;6:pl1. doi: 10.1126/scisignal.2004088.
21. Cerami E, Gao J, Dogrusoz U, Gross BE, Sumer SO, Aksoy BA, *et al*. The cBio cancer genomics portal: An open platform for exploring multidimensional cancer genomics data. Cancer Discov 2012;2:401–404. doi: 10.1158/2159-8290.CD-12-0095.
22. Szklarczyk D, Gable AL, Nastou KC, Lyon D, Kirsch R, Pyysalo S, *et al*. The STRING database in 2021: Customizable protein-protein networks, and functional characterization of user-uploaded gene/measurement sets. Nucleic Acids Res 2021;49:10800. doi: 10.1093/nar/gkab835.
23. Aran D, Hu Z, Butte AJ. xCell: Digitally portraying the tissue cellular heterogeneity landscape. Genome Biol 2017;18:220. doi: 10.1186/s13059-017-1349-1.
24. Martincorena I, Raine KM, Gerstung M, Dawson KJ, Haase K, Van Loo P, *et al*. Universal patterns of selection in cancer and somatic tissues. Cell 2017;171:1029–1041. e21. doi: 10.1016/j.cell.2017.09.042.
25. Han Z, Mo R, Cai S, Feng Y, Tang Z, Ye J, *et al*. Differential expression of E2F transcription factors and their functional and prognostic roles in human prostate cancer. Front Cell Dev Biol 2022;10:831329. doi: 10.3389/fcell.2022.831329.
26. McNair C, Xu K, Mandigo AC, Benelli M, Leiby B, Rodrigues D, *et al*. Differential impact of RB status on E2F1 reprogramming in human cancer. J Clin Invest 2018;128:341–358. doi: 10.1172/JCI93566.
27. Xiao J, Sun F, Wang YN, Liu B, Zhou P, Wang FX, *et al*. UBC9 deficiency enhances immunostimulatory macrophage activation and subsequent antitumor T cell response in prostate cancer. J Clin Invest 2023;133:e158352. doi: 10.1172/JCI158352.
28. Ciccarelli C, Di Rocco A, Gravina GL, Mauro A, Festuccia C, Del Fattore A, *et al*. Disruption of MEK/ERK/c-Myc signaling radiosensitizes prostate cancer cells in vitro and in vivo. J Cancer Res Clin Oncol 2018;144:1685–1699. doi: 10.1007/s00432-018-2696-3.
29. Li S, Fong KW, Gritsina G, Zhang A, Zhao JC, Kim J, *et al*. Activation of MAPK signaling by CXCR7 leads to enzalutamide resistance in prostate cancer. Cancer Res 2019;79:2580–2592. doi: 10.1158/0008-5472.CAN-18-2812.
30. Niehrs C, Keller R, Cho KW, De Robertis EM. The homeobox gene goosecoid controls cell migration in Xenopus embryos. Cell 1993;72:491–503. doi: 10.1016/0092-8674(93)90069-3.
31. Garnis C, Buys TP, Lam WL. Genetic alteration and gene expression modulation during cancer progression. Mol Cancer 2004;3:9. doi: 10.1186/1476-4598-3-9.
32. Giannareas N, Zhang Q, Yang X, Na R, Tian Y, Yang Y, *et al*. Extensive germline-somatic interplay contributes to prostate cancer progression through HNF1B co-option of TMPRSS2-ERG. Nature Commun 2022;13:7320. doi: 10.1038/s41467-022-34994-z.
33. Hahn WC, Weinberg RA. Rules for making human tumor cells. N Engl J Med 2002;347:1593–1603. doi: 10.1056/NEJMra021902.
34. Shrestha M, Wang DY, Ben-David Y, Zacksenhaus E. CDK4/6 inhibitors and the pRB-E2F1 axis suppress PVR and PD-L1 expression in triple-negative breast cancer. Oncogenesis 2023;12:29. doi: 10.1038/s41389-023-00475-1.
35. Nakajima R, Zhao L, Zhou Y, Shirasawa M, Uchida A, Murakawa H, *et al*. Deregulated E2F activity as a cancer-cell specific therapeutic tool. Genes (Basel) 2023;14:393. doi: 10.3390/genes14020393.
36. Kassab A, Gupta I, Moustafa AA. Role of E2F transcription factor in oral cancer: Recent insight and advancements. Semin Cancer Biol 2023;92:28–41. doi: 10.1016/j.semcancer.2023.03.004.
37. Song Z, Cao Q, Guo B, Zhao Y, Li X, Lou N, *et al*. Overexpression of RACGAP1 by E2F1 promotes neuroendocrine differentiation of prostate cancer by stabilizing EZH2 expression. Aging Dis 2023;Online ahead of print. doi: 10.14336/AD.2023.0202.
38. Mandigo AC, Shafi AA, McCann JJ, Yuan W, Laufer TS, Bogdan D, *et al*. Novel oncogenic transcription factor cooperation in RB-deficient cancer. Cancer Res 2022;82:221–234. doi: 10.1158/0008-5472.CAN-21-1159.
39. Kishan AU, Sun Y, Hartman H, Pisansky TM, Bolla M, Neven A, *et al*. Androgen deprivation therapy use and duration with definitive radiotherapy for localised prostate cancer: An individual patient data meta-analysis. Lancet Oncol 2022;23:304–316. doi: 10.1016/S1470-2045(21)00705-1.
40. Wala J, Nguyen P, Pomerantz M. Early treatment intensification in metastatic hormone-sensitive prostate cancer. J Clin Oncol 2023;52:3584–3590. doi: 10.1200/JCO.23.00723.
41. Feng J, Lian Z, Xia X, Lu Y, Hu K, Zhang Y, *et al*. Targeting metabolic vulnerability in mitochondria conquers MEK inhibitor resistance in KRAS-mutant lung cancer. Acta Pharm Sin B 2023;13:1145–1163. doi: 10.1016/j.apsb.2022.10.023.
42. Schreuer M, Meersseman G, Van Den Herrewegen S, Jansen Y, Chevolet I, Bott A, *et al*. Quantitative assessment of BRAF V600 mutant circulating cell-free tumor DNA as a tool for therapeutic monitoring in metastatic melanoma patients treated with BRAF/MEK inhibitors. J Transl Med 2016;14:95. doi: 10.1186/s12967-016-0852-6.
43. Elkrief A, Odintsov I, Markov V, Caeser R, Sobczuk P, Tischfield SE, *et al*. Combination therapy with MDM2 and MEK inhibitors is effective in patient-derived models of lung adenocarcinoma with concurrent oncogenic drivers and MDM2 amplification. J Thorac Oncol 2023;18:1165–1183. doi: 10.1016/j.jtho.2023.05.007.
44. Sun K, Jin L, Karolová J, Vorwerk J, Hailfinger S, Opalka B, *et al*. Combination treatment targeting mTOR and MAPK pathways has synergistic activity in multiple myeloma. Cancers (Basel) 2023;15:2373. doi: 10.3390/cancers15082373.

How to cite this article: Ge Y, Ma S, Zhou Q, Xiong ZZ, Wang YN, Li L, Chao Z, Zhang JB, Li TF, Wu ZX, Gao Y, Qu GY, Xi ZR, Liu B, Wu X, Wang ZH. Oncogene goosecoid is transcriptionally regulated by *E2F1* and correlates with disease progression in prostate cancer. Chin Med J 2024;137:1844–1856. doi: 10.1097/CM9.0000000000002865